

First Sources in Infrared Light: Stars, Supernovae and Miniquasars

Asantha Cooray¹ and Naoki Yoshida^{2,3}

¹*Theoretical Astrophysics, California Institute of Technology, MS 130-33, Pasadena, CA 91125, USA*

²*Division of Theoretical Astrophysics, National Astronomical Observatory Japan, Mitaka, Tokyo 181-8588, Japan*

³*Department of Physics and Astrophysics, Nagoya University, Nagoya 464-8602, Japan*

29 October 2018

ABSTRACT

The cosmic infrared background (IRB) at wavelengths between $1 \mu\text{m}$ and $3 \mu\text{m}$ provides a useful probe of early star-formation prior to and during reionization. To explain the high optical depth to electron scattering, as measured by the Wilkinson Microwave Anisotropy Probe (WMAP), one requires significant star-formation activity at redshifts 10 and higher. In addition to massive stars, the IRB flux may be contributed by a population of early miniquasars. We study the relative contributions from first stars, supernovae and quasars to the IRB for reasonable star formation rates at high redshift. If miniquasars radiate efficiently at the Eddington-limit, current background measurements limit the fraction of mass in first stars that is converted to seed black holes to be roughly less than 10%. In the case of supernovae, though an individual supernova is much brighter than the progenitor star, due to the shorter lifetime of order few months, the fractional contribution to the IRB remains at a level of 10% and below when compared to the same contribution from stars. The bright supernovae may, however, be directly detectable by future large ground-based and space telescopes.

Key words: infrared:general — stars:formation — cosmology:observations — diffuse radiation

1 INTRODUCTION

The Wilkinson Microwave Anisotropy Probe (WMAP) has provided strong evidence for an optical depth for electron scattering of 0.17 ± 0.04 based on the large scale polarization pattern related to rescattering of Cosmic Microwave Background (CMB) photons (Kogut et al. 2003). If the reionization process is described as instantaneous and homogeneous, the measured optical depth implies a reionization redshift of $\sim 17 \pm 5$ in a spatially flat universe. Interestingly, the derived redshift for reionization is at the high end of expectations in models in which stellar populations are dominant reionization sources (e.g., Cen 2003; Fukugita & Kawasaki 2003; Venkatesan, Tumlinson & Shull 2003; Wyithe & Loeb 2003; Sokasian et al. 2004). Thus, in some of these models, primordial stars, the so-called Population III stars, are assumed to be rather massive and hence have a large UV photon emission rate, as suggested by recent theoretical studies (e.g. Abel, Bryan & Norman 2002; Bromm, Coppi & Larson 2002; Bromm, Kudritzki & Loeb 2001; Schaerer 2002, 2003).

The formation of such massive stars in the early universe has many important cosmological implications (e.g.,

Carr, Bond, & Arnett 1984; Oh, Cooray Kamionkowski 2003; Yoshida, Bromm & Hernquist 2004). Because radiation below the Lyman-limit is absorbed by neutral hydrogen, luminous sources at redshifts 10 and higher are generally seen only in the near-IR band. In particular, if Pop III stars are formed primarily at redshifts between 10 and 30, they are expected to contribute to the infrared background (IRB) light at wavelengths between 1 and $5 \mu\text{m}$ at present epoch (Bond, Carr & Hogan 1986). Recent estimates based on theoretical models suggest that a large fraction of the IRB total intensity may indeed be due to these stars (Santos et al. 2002; Salvaterra & Ferrara 2003; Cooray et al. 2004). A substantial IRB could arise from the Pop III stars not only due to the direct emission associated with these stars, but also due to indirect processes that lead to free-free and Lyman- α emission from the ionized nebulae, or HII regions, surrounding these stars.

Observationally, about 20-40% of the near-IR flux (between $\sim 1 \mu\text{m}$ and $3 \mu\text{m}$) has been resolved by point sources (Cambrésy et al. 2001; Totani et al. 2001); while J- and K-band source counts go down to AB-magnitudes of ~ 28 and 25, respectively, the cumulative surface brightness con-

verges by a magnitude around 23, say, in the K-band (see for a review of existing data by Pozzetti & Madau 2000). The missing IR flux could be either due to a high- z population of galaxies, such as the proto-galaxy population related to first stars (Santos et al. 2002; Salvaterra & Ferrara 2003), or a population of low surface brightness galaxies at nearby redshifts. While there still remains uncertainties, one can potentially understand the presence of first luminous sources and some details related to their population, such as the number density, by characterizing the background light from optical to infrared at wavelengths of a few micron. In this wavelength range, final products of these massive stars are also expected to contribute to IRB, in addition to the direct emission from stars; Radiation from supernovae and primordial black holes, in the form of miniquasars, may be significant sources of emission. The role of final products in contributing to the IRB, relative to the progenitor stars, depends on the initial mass function of the first stars.

As the end state of a massive star above $\sim 260 M_{\odot}$ is a complete collapse to a black hole (Heger & Woosley 2002), if the first stellar population is extremely top-heavy with all mass above this limit, then one expects roughly a similar number density of black holes as that of stars. These black holes grow via accretion and/or mergers and may partly be responsible for early reionization if they radiate as mini-quasars (Haiman & Loeb 1998; Madau et al. 2004; Ricotti & Ostriker 2003). The UV output from such quasars, if not absorbed heavily by the surrounding torii, can contribute both to reionization and to the IR flux as viewed today. The unresolved soft X-ray background at energies between 0.5 and 2 keV may rule out a large density of miniquasars at high redshifts as required to reionize the universe from the quasar emission alone (Dijkstra, Haiman & Loeb 2004) unless reionization by miniquasars, within uncertainties of models used in Dijkstra et al., is completed by a redshift of 20. Here, we suggest that if all massive stars are eventually converted to black holes and accrete efficiently at the Eddington-rate (as would be the case if miniquasars are responsible for eventual reionization of the Universe), then the IR background is overproduced. A more realistic situation could be that the mass function is broad, and only a small fraction of the total initial stellar mass is converted to black holes; current understanding of the IRB may limit the mass fraction of stars above $260 M_{\odot}$ to a level less than 10%. This constraint can be relaxed if miniquasars radiate less efficiently below the Eddington-limit; such a scenario may be viable if stellar sources dominate the UV photon production and are, thus, responsible for reionization, though some fraction of stellar mass is converted to miniquasars.

The initial mass function of the first stars could potentially be dominated by stars with masses in the range between 140 and $260 M_{\odot}$. In this case, the final product will be a complete disruption of the star via the pair-instability process (Heger & Woosley 2002). In the case of such massive stars, in general, one expects a typical supernovae to be much brighter than the star, suggesting that a modest contribution to the IRB could come from supernovae, when compared to the fractional contribution from stellar emission alone. However, though supernovae are in fact brighter than

an average star, the duration over which most optical flux is emitted is relatively smaller. We show that this results in a small but non-negligible contribution to the IRB from supernovae associated with massive Pop III stars. While the background contribution is smaller, these supernovae are likely to be detectable directly in deep IR images above $1 \mu\text{m}$ down to AB-magnitude limits at the level of 26 and fainter.

In the next section, we discuss the contribution to IRB from the first generation of stars, supernovae, and mini-quasars under the assumption that the early stellar population is dominated by very massive stars. In the case of supernovae, we will suggest that, while the relative contribution to the IRB may be lower, individual detections may be possible with deep-IR imaging. We also suggest that the IR background itself may be used to constrain the presence of early mini-quasars. Throughout the paper, we make use of a Λ CDM cosmological model consistent with current data (e.g., Tegmark et al. 2004) with $\Omega_m = 1 - \Omega_{\Lambda} = 0.3$, $h = 0.7$, $\Omega_b = 0.04$, the spectral index of the primordial power $n = 1$, and a normalization for the matter power spectrum with $\sigma_8 = 0.9$.

2 FIRST-SOURCES IN THE IR BACKGROUND

Our calculations of the first-source contribution to the IRB follow previous calculations in the literature related to the stellar contribution to the IRB (Santos et al. 2002; Salvaterra & Ferrara 2003; Cooray et al. 2004; Kashlinsky et al. 2004). These studies involve two basic ingredients: (1) the rate at which the volume density of first-sources evolves and (2) the flux spectrum. We extend these calculations to supernovae and miniquasars, which have been so far ignored in previous estimates, under the assumption that (1) the supernova rate in the early universe traces that of the star formation and (2) the formation rate of miniquasars is simply related to the formation rate of seed black holes, taken to be proportional to the star-formation, and to a model description for accretion. We use a simple model to describe the spectrum and the light curve of supernovae following results from Heger et al. (2002).

For miniquasars, we make use of the average spectrum of quasars derived by Sazonov et al. (2004) using fits to observational data over the range of wavelengths corresponding to X-rays and optical and, thereafter, using models to describe the emission, such as in the IR band. While the spectral shape is well defined in the average sense for observed luminous quasars at redshifts less than ~ 6 , it is unclear to which extent this spectrum can be applied to miniquasars at redshifts greater than 10 and with masses in the range of $10^2 M_{\odot}$ to $10^4 M_{\odot}$. At energies below 13.6 eV, the Sazonov et al. (2004) spectrum, νF_{ν} , scales as $\nu^{-0.7}$ though expectations for miniquasars are that the spectrum is harder such that νF_{ν} is a constant (Madau et al. 2004; Dijkstra, Haiman & Loeb 2004). Regardless of the exact shape of the spectrum, there is also an uncertainty with respect to the overall normalization, or the total luminosity of a given miniquasar. Here, we make the assumption that miniquasars radiate efficiently at the maximum allowed by the

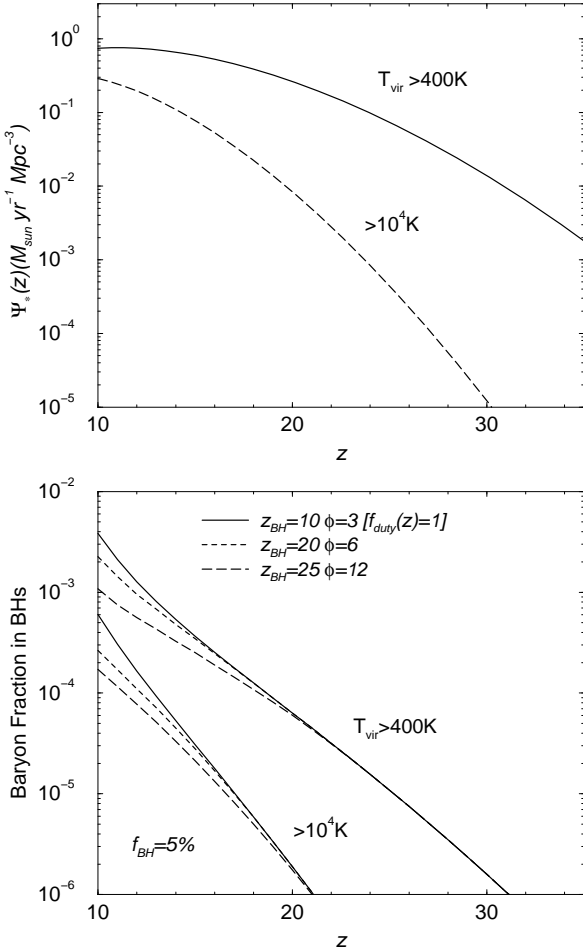


Figure 1. *Top panel:* The global star formation rate density at redshifts greater than 10 calculated based on the Press-Schechter (PS) mass function with a minimum virial temperature of 400 K (top line) and 10^4 K (bottom line). *Bottom panel:* The baryon fraction in black holes as a function of redshift, under the assumption that the star-formation history related to the seed population follows the two curves shown in the top panel. We have assumed a 5% of the mass in stars are converted to seed black holes. The three curves in each of the star-formation models follow a model description related to the duty cycle of accretion growth following Ricotti & Ostriker (2003) with parameters shown on the figure (see Section 2.1 for a discussion).

Eddington-limit. In making this choice, we are guided by observations of quasars out to redshifts of 6 which indicate maximal emission at the Eddington-limit. These quasars are more massive and more luminous than the miniquasar counterparts at high redshifts. It is likely that the miniquasar emission is submaximal. The limits we derive here on the fraction of miniquasars present during the reionization era should, thus, only be taken as a conservative limit on the low end given the current state of knowledge on the IR background.

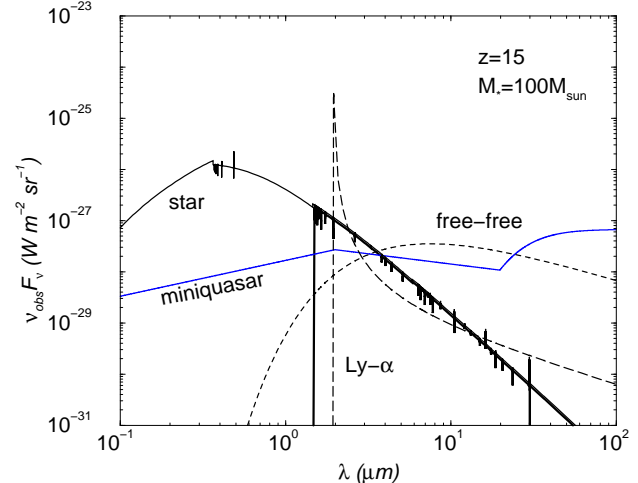


Figure 2. The flux spectrum, νF_ν , of a $100 M_\odot$ star at a redshift of 15 as observed today as a function of the observed wavelength. In addition to the stellar spectrum (solid line), we also show the nebular Lyman- α emission (long-dashed line) and free-free (dashed line) of the ionized HII region surrounding the star, when the UV end of the stellar-spectrum (thin solid line) is used to ionized the surrounding medium. The spectrum follows from model calculations by Santos et al. (2002). We assume all ionizing photons are absorbed by the nebula. For comparison, we also show the spectrum of a miniquasar of the same mass ($M_{BH,seed} = 100 M_\odot$) at a redshift of 15, as viewed today (solid line labeled 'miniquasar'). The spectrum is computed using the template derived in Sazonov et al. (2004). The bump around $\sim 100\mu\text{m}$ shows a possible contribution from thermal reradiation of UV photons by dust. While the overall flux from a miniquasar is similar to that of a star, we argue that the contribution to IRB from miniquasars could dominate stars because of their larger number density; quasars live longer than massive stars.

2.1 Formation rates and background flux

In order to calculate the formation rate of first stars and the subsequent supernovae or seed black holes, we use an analytical description for halo formation following the Press-Schechter formalism (Press & Schechter 1974). We write the star-formation rate as

$$\psi_*(z) = \eta \frac{\Omega_b}{\Omega_m} \frac{d}{dt} \int_{M_{\min}}^{\infty} dM M \frac{dn}{dM}, \quad (1)$$

where M_{\min} is the minimum mass of halos in which gas can cool, and we take the star-formation efficiency $\eta = 0.4$. We consider two cases for M_{\min} with a minimum virial temperature of 400 K, involving molecular hydrogen (e.g., Tegmark et al. 1997), and 10^4 K involving atomic hydrogen line cooling (Barkana & Loeb 2001). The respective star-formation rates are shown in Fig. 1 (top panel). We mention that, although more detailed modeling of early star formation is available (e.g. Hernquist & Springel 2003; Yoshida et al. 2003), the overall feedback effects from mini-quasars on star-formation are still uncertain (see, e.g. Machacek, Bryan, Abel 2003). We thus prefer using the model described above for the sake of simplicity. Note that the scenario with a minimum tem-

perature $T_{\text{vir}} = 400\text{K}$ likely provides a possible maximal star-formation rate.

Given the rate of formation of stars, we can write the emissivity per comoving unit volume at a certain wavelength λ as a function of redshift z as

$$j_{\nu}^c(z) = \frac{l_{\nu}}{4\pi} \langle t_{\text{age}} \rangle \psi_{*}(z), \quad (2)$$

where l_{ν} is the luminosity per source mass as a function of frequency and t_{age} is the lifetime over which this flux is emitted; for a single source at a redshift of z with a source mass M_s , such as a first-star, the total Luminosity, as a function of frequency, is $L_{\nu} = l_{\nu} M_s$ and the observed flux today is $F_{\nu} = L_{\nu}(1+z)/[4\pi d_L^2]$, where d_L is the cosmological luminosity distance out to a redshift of z .

The cumulative background is obtained by integrating the emissivity over redshift, yielding the specific intensity I_{ν}

$$v_{\text{obs}} I_{\nu} = c \int_0^{\infty} dz \frac{dr}{dz} \nu(z) \frac{j_{\nu}^c(z)}{1+z}, \quad (3)$$

where v_{obs} is the observed frequency, $\nu(z) = (1+z)v_{\text{obs}}$ is the redshift scaling of the frequency, and r is the proper distance such that $dr/dz = 1/[(1+z)H(z)]$ when the expansion rate for adiabatic cold dark matter cosmological models with a cosmological constant and a flat space-time geometry is $H^2(z) = H_0^2[\Omega_m(1+z)^3 + \Omega_{\Lambda}]$. In terms of the individual source fluxes, and their comoving number density $n_s(z)$, the specific intensity of the background can also be written as $v_{\text{obs}} I_{\nu} = \int dz (dV/d\Omega dz) \nu(z) F_{\nu}(z) n_s(z)$, where $n_s(z) = \langle t_{\text{age}} \rangle \psi_{*}(z)/M_s$ and $(dV/d\Omega dz)$ is the cosmological volume element given by $d_L^2/(1+z)^2 dr/dz$, in terms of the luminosity distance. This expression and equation (3) are equivalent.

We use the same formalism to compute the background radiation intensities from stars, supernovae and miniquasars. We assume that the supernovae rate follows that of the star-formation. For miniquasars, we follow Ricotti & Ostriker (2003) and write the growth rate of black holes as

$$\dot{\omega}_{\text{BH}}(z) = \dot{\omega}_{\text{ac}}(z) + \dot{\omega}_{\text{seed}}(z), \quad (4)$$

where the two terms represent the growth of black holes via accretion, $\dot{\omega}_{\text{ac}}$, and the formation rate of seed black holes, $\dot{\omega}_{\text{seed}}$. The over-dot represents the derivative with respect to proper time. We ignore black hole removal process, such as through ejection from proto-galaxies, and take $\dot{\omega}_{\text{seed}}(z) = f_{\text{BH}} \psi_{*}(z)$ where $\psi_{*}(z)$, the star-formation rate, is given by equation (1), and f_{BH} represents the overall fraction of stars converted to seed black holes. We model growth related to accretion as $\dot{\omega}_{\text{ac}}(z) = f_{\text{duty}}(z) \omega_{\text{BH}}(z)/t_{\text{Edd}}$, where Eddington time is set to be a constant at 10^8 years and use the same parametrization in Ricotti & Ostriker (2003) for f_{duty} such that $f_{\text{duty}}(z) = [(1+z)/z_{\text{BH}}]^{\phi}$ with the condition that $f_{\text{duty}}(z) \leq 1$ based on the definition that $f_{\text{duty}} = t_{\text{on}}/(t_{\text{on}} + t_{\text{off}})$ where t_{on} and t_{off} are time intervals over which the blackhole accretes and does not accrete, respectively. At the low end, following Ricotti & Ostriker (2003), we set $f_{\text{duty}}(z) > 10^{-3}$ to be consistent with both the AGN fraction at $z \sim 3$ and today (Steidel et al. 2002). In Fig. 1 (bottom panel), we show $\omega_{\text{BH}}(z)$ normalized to the baryon density and assuming $f_{\text{BH}} = 0.05$ for a variety of

models related to f_{duty} with parameters as labeled on the figure.

2.2 Source Spectra

The spectrum of stellar emission is computed as in Santos et al. (2002), including the nebular and free-free emission. For the miniquasar spectrum, we make use of the model of Sazonov et al. (2004). We assume that the Sazonov et al.'s template for the average quasars also applies to miniquasars. In Fig. 2, we compare the spectrum of a typical star with $100M_{\odot}$ and that of a miniquasar at a redshift of 15, as viewed today. Here we plot $\nu_{\text{obs}} F_{\nu}$ (in units of $\text{W m}^{-2} \text{sr}^{-1}$). The miniquasars are assumed to radiate at the Eddington-limit such that the total integrated luminosity over the range from X-rays to far-infrared is $\approx 1.3 \times 10^{38}$ ergs s^{-1} ($\text{M}_{\text{BH}}/\text{M}_{\odot}$), though, as discussed in Section 2, it is likely that the miniquasar emission is submaximal. Also, at observed wavelengths below $\sim 2 \mu\text{m}$, corresponding to redshifted Lyman- α emission, the miniquasars flux spectrum νF_{ν} scales as $\nu^{-0.7}$. For miniquasars, it could be that the spectrum is harder (in terms of energy), such that the expectation is that νF_{ν} is constant at energies above 13.6 eV (Madau et al. 2004; Dijkstra, Haiman & Loeb 2004). This will result in a flatter spectrum, as observed today, from optical/UV to IR wavelengths. As shown in Fig. 2, we assume that stellar emission is responsible for reionization of the universe; the Lyman- α emission is related to ionizing photons that are first absorbed by the neutral medium and are re-emitted during recombinations. In the case of miniquasars, we do not consider UV absorption as we have implicitly assumed that the surrounding medium is already ionized by stars preceding the formation of a miniquasar in or near that location. We will comment on this later in the discussion. As shown in Fig. 2, the level of the incident flux from a typical star and a miniquasar is similar.

The spectrum and light curve for Population III supernovae were calculated by Heger et al. (2002). In these calculations, the relevant IR emission, as observed today, characterizing the peak of the light curve, is delayed a month or so from the initial explosion and the resulting shock break out. The latter includes emission at short wavelengths, below the Lyman limit, in the supernova frame, which is likely be absorbed by the intergalactic medium at epochs prior to complete reionization. The peak of the light curve extends over a month at most. In order to make a reasonable estimate of the supernovae contribution to the IRB, we use the peak emission and its duration only and ignore detailed aspects of the light curve when fluxes drop below more than a factor of 10 from the peak emission. Including the full light curve only leads to minor corrections at a few percent level. While the peak emission is flat such that λF_{λ} is a constant in the estimate by Heger et al. (2002), to study any departures, we also allow the spectrum to vary as $\lambda F_{\lambda} \propto \lambda^{\alpha}$ with α between -0.5 and 0.5, with $\alpha = 0$ as the fiducial case. When varying the spectral shape, we renormalize such that the total flux, or the luminosity, remains constant in the rest wavelengths between 10^2\AA and 10^4\AA corresponding to the UV and optical regimes. Here, again, we assume that the

surrounding medium is reionized by stellar emission before the supernova explosion and that the rest UV emission is not absorbed. The reionization by supernovae may not be important as the time scale over which the rest UV emission is expected is significantly smaller than that of a star (a month vs. a few million years, respectively). Note that the supernova spectrum of a Pop III star is highly uncertain in terms of spectral shape at the UV end and more numerical models are needed to further address the extent to which supernovae may be an important source of ionizing photons. A more likely scenario involving Pop III supernovae is the one described in Oh, Cooray & Kamionkowski (2003), where the blast wave propagates to the dense ionized IGM and heats the electrons to a substantial temperature which subsequently cools via inverse Compton-scattering off of the cosmic microwave background, similar to the same effect related to hot electrons in galaxy clusters (the Sunyaev-Zel'dovich effect; Sunyaev & Zel'dovich 1980).

2.3 Infrared background

We summarize our results in Fig. 3, where we show the contributions to total IRB light from stars, supernovae and miniquasars. In the case of stars, we divide the contribution to the three main components; direct emission from stars, Lyman- α recombination radiation from the ionized patch, and the free-free component related to electron-ion scatterings within each ionized patch surrounding these stars. Our calculations related to the IRB light due to stars are consistent with those in Santos et al. (2002) and Salvaterra & Ferrara (2003), except that here we have assumed a slightly different redshift limit to the first generation of stars at a value of 10 instead of values such as 7 and 8 used in those calculations that are aimed at explaining the total missing content.

Our results suggest that, while the emission associated with stars can explain most of the IRB intensities, the fractional contribution from supernovae is an order of magnitude smaller than the stellar emission contribution. The relative difference between stars and supernovae is easily understood based on the typical flux from a star vs. a supernovae and the ages over which these fluxes are emitted. For example, typical $\sim 200 M_{\odot}$ star at a redshift of 20 has a flux, ignoring Lyman- α emission, of order $\sim 10^{-35}$ ergs $cm^{-2} s^{-1} Hz^{-1}$ ($\sim 10^{-3}$ nJy or $m_{AB} \sim 39$), while the peak flux of the supernovae at the same redshift is at the level of \sim few times 10^{-30} ergs $cm^{-2} s^{-1} Hz^{-1}$ ($\sim 1 \mu$ Jy or $\sim m_{AB} \sim 26$). Even if all the stars at redshifts greater than 10 die as supernovae, though the instant flux is greater, the total output of $(F_{\nu} t_{age})$ from supernovae is smaller than stars as the stellar emission lasts over a million years while the peak flux from supernovae lasts just over a month or so. Thus, the apparent high ratio of the *peak* luminosity is largely compensated by the age difference so that the typical ratio of a supernova to stellar flux remains at most at the level of ~ 0.1 .

Note that the stellar contribution to the IRB also includes a substantial fraction from the Lyman- α emission of absorbed ionizing UV photons during subsequent recombinations. We have not included such a contribution from in-

dividual Pop III supernovae because of uncertainty in the supernovae spectrum at the UV end. Note also that regions surrounding supernovae is likely to have been ionized by the progenitor stars. Even if the IGM between protohalos are partly ionized, the resulting Lyman- α emission is expected to be suppressed relative to the case of stellar sources. This can be understood from the fact that the Lyman- α spectrum, as a function of frequency, can be written as $l_{Ly\alpha}(\nu) = qh \nu_{Ly\alpha} \phi(\nu)$, where $\phi(\nu)$ is the fit to the Lyman- α profile of Loeb & Rybicki (1999) by Santos et al. (2002) and the production rate of Lyman- α photons from recombinations is $q \sim 0.6(t_{age})\alpha_B(T)n_e^2 \dot{R}$, where n_e is the electron density of the surrounding medium, $\alpha_B(T)$ is the case-B recombination coefficient for HI as a function of the electron temperature T , and \dot{R} is the ionizing photon production rate (see Santos et al. 2002 for details). To estimate \dot{R} , we assume that the supernovae spectrum is flat (in rest νF_{ν} below the Lyman-limit) and given the uncertainty in spectral shape, we take the production rate to be that associated with ionizing photons at the wavelength corresponding to the Lyman-limit. The model related to stars is shown in Fig. 2, where the unabsorbed spectrum peaks at a wavelength of $\sim 300 \text{ \AA}$ (rest frame). The difference in flux, as suggested above, translates to a stellar-to-supernovae ionizing photon production rate difference of $\sim 10^{-5}$ to 10^{-6} . This should then be compared to the ratio of ages, which is again, $\sim 10^7$ between stars and supernovae. Furthermore, in the case of supernovae, the Lyman- α radiation is more likely to be associated with tenuous IGM with density $\sim 10^{-7}(1+z)^3 \text{ cm}^{-3}$ compared to dense nebulae surrounding stars (with density 10^4 cm^{-3}). This lowers the Lyman- α flux by another factor of 10^6 relative to that of stars, resulting in an overall reduction of 10^{-5} to 10^{-7} in the Lyman- α contribution from stars to supernovae. Thus, it is unlikely that the difference between predicted supernovae background and the missing IRB flux can be reconciled with the expected increase associated with Lyman- α emission if the UV emission from supernovae are absorbed during the reionization process.

Intriguingly, redshifted light from early miniquasars can explain the IR excess at wavelengths around $1 \mu\text{m}$, as shown in Fig 3(c). In fact, if *all* stars collapse to become seed black holes, we find that the flux from miniquasars that grow down to $z \sim 10$ will *exceed* the measured IR fluxes by an order of magnitude or more. A fractional contribution of $\sim 5\%$ to 10% of initial stellar mass to seed black holes appears consistent with observations. This is based on our assumption that the miniquasars are radiating efficiently at the maximum given by the Eddington-limit. As discussed at the beginning of Section 2, the extent to which such an assumption, based on observations of luminous quasars at redshifts less than 6, applies to high-redshift miniquasars is unclear. If the radiation from miniquasars, with masses between $10^2 M_{\odot}$ and $10^4 M_{\odot}$, is submaximal, the derived limit on the fractional contribution from $\sim 5\%$ to 10% can be increased. Thus our result should be considered as a *weak* constraint.

Since the typical stellar age is $\sim 2 \times 10^6$ years (Bromm, Kudritzki & Loeb 2001), at a redshift of around 10, using the highest star-formation rate in Fig. 1 (top panel), one finds a typical density of order a few times $10^6 M_{\odot} \text{ Mpc}^{-3}$ in stars.

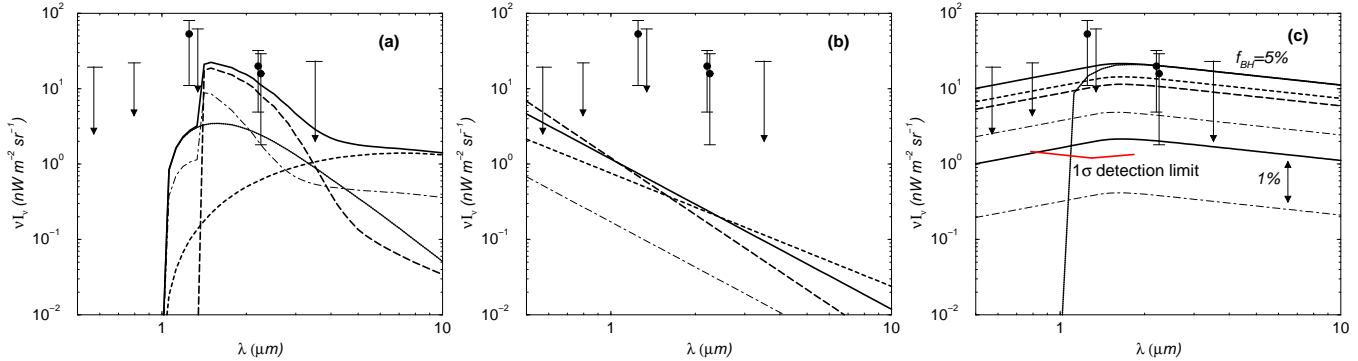


Figure 3. The cosmic infrared background due to Population III stars (a), first supernovae (b), and miniquasars (c). The data points and upper limits are related to unexplained IRB intensities from measurements and calculations in the literature. For reference, we show the same observational data as the ones plotted in Fig. 6 of Santos et al. (2002; the measurements at $1.25\ \mu\text{m}$ and $2.2\ \mu\text{m}$ from Cambrésy et al. 2001; upper limit at $1.25\ \mu\text{m}$, a second measurement at $2.2\ \mu\text{m}$, and a upper limit at $3.5\ \mu\text{m}$ from Wright & Johnson (2001); upper limits at $0.6\ \mu\text{m}$ and $0.8\ \mu\text{m}$ from Bernstein, Freedman & Madore 2002). Note that these background measurements are corrected for the known contribution from Galactic stars and galaxies down to magnitude limits of order 25 (see, Santos et al. 2002 for further details). In the case of stellar contribution to the IRB shown in Panel (a), we show the contribution from stellar emission alone (dotted line), associated Lyman- α emission due to recombinations in the ionized patches surrounding individual stars (long-dashed line), the free-free emission due to electron/ion scattering within individual ionized patches (dashed line), and the sum of these three contributions (thick solid line). These curves make use of the star formation rate (SFR) density based on the PS mass function with a minimum temperature for collapse of 400 K; for illustration, the bottom dot-dashed curve is the total contribution to the IR background in the case where minimum temperature is set at 10^4 K. In the case of supernovae, in Panel (b), the three curves assume flux spectra for supernovae emission, $\lambda F_\lambda \propto \lambda^\alpha$ with $\alpha = 0$ (solid line), -0.5 (dashed line), 0.5 (long-dashed line); The curves are normalized such that the total flux or total luminosity is same in the UV to optical bands (see Section 2.2 for details). The top curves assume PS mass function to calculate the SFR with $T_{\text{vir}}=400\text{K}$, but the case with $T_{\text{vir}}=10^4\text{K}$, for $\alpha = 0$, is shown as a dot-dashed line. In the case of miniquasars in Panel (c), we consider three models for the accretion duty cycle as plotted in Fig. 1 (bottom panel) with parameters given in that figure and plotted as top three curves with thick lines when $T_{\text{vir}}=400\text{K}$. The middle dot-dashed curve is for the case corresponding to the solid line but with $T_{\text{vir}}=10^4\text{K}$. These curves assume a seed black hole mass fraction, f_{BH} , of 5%. For reference, we also show the range implied by the solid line and the dot-dashed line, with thin bottom lines, when this fraction is reduced to 1%. Note that we have assumed the case that no UV photons are absorbed by the IGM surrounding these miniquasars. The solid curve labeled '1 σ detection limit' is the extent to which the optical to near IR background can be established, over the wavelength regime indicated by the curve, using a low resolution spectrometer on a proposed rocket experiment.

From the bottom panel of Fig. 1, one finds that the density of miniquasars is typically $\sim 10^8\ M_\odot\ \text{Mpc}^{-3}$. This apparent increase in miniquasar density, however, is compensated by the fact that the miniquasars flux, at relevant wavelengths, is roughly an order of magnitude smaller than that of a typical very massive star (see Fig. 2). The exact numerical calculation reveals that the miniquasars do dominate the background if the fraction of stars converted to seed black holes is large. In other words, the IRB offers a useful way to constrain the presence and abundance of miniquasars at $z > 10$; under our assumption, an initial mass fraction of black holes, relative to stars, of order 10% and below seems consistent with current observations.

This conclusion may indeed be strengthened if ionizing photons from miniquasars are absorbed by the neutral IGM; if absorbed, we expect some fraction of the energy to be reradiated in the form of the Lyman- α line and to increase the IRB at the corresponding frequencies such that the upper bound on the black hole mass fraction is further reduced. On the other hand, as discussed in the case for supernovae above, we do not expect the Lyman- α radiation to be significant as long as the dense nebula surrounding quasar is fully ionized already by the stellar emission prior to the formation of the miniquasar. The miniquasar emission can ionize

the IGM beyond the nebula, but due to the lower density, recombinations are unlikely to be significant such that the Lyman- α emission is suppressed relative to the case where stars form and ionize dense nebulae surrounding such stars initially.

Our suggestion that the seed mass fraction must be below 10%, assuming efficient radiation at the Eddington-limit, also suggests that the universe cannot be reionized by early quasars alone. For reference, in Fig. 3, we show the model in which the UV photons from miniquasars are absorbed by neutral IGM during the reionization process (thick dot-dashed line in the figure). Integrating the UV light below the hydrogen Lyman-limit, we find a ratio of number density of photons relative to mean density of baryons at the level of 0.3 at $z \sim 10$; to fully reionize, one would expect this ratio to be at least unity or as high as 25 as the recombinations are important at high redshifts. In Oh, Cooray & Kamionkowski (2003), it was estimated that $25 \pm 12(f_{\text{esc}}/0.3)^{-1}(\tau_e/0.12)(C_{\text{II}}/4)$ photons per baryon are needed to explain an optical depth to reionization of 0.12 when the clumping factor of ionized gas C_{II} is 4 and the escape fraction of ionized photons is 0.3, consistent with other estimates (e.g., Dijkstra, Haiman & Loeb 2004). Note also that ionization by a combination of hard X-rays and sec-

ondary electrons does not lead to complete ionization, as argued by Madau et al. (2004).

Our constraint on the total mass fraction of miniquasar-seed blackholes is independent of similar suggestions in the literature, for example, based on the unresolved X-ray background (Dijkstra, Haiman & Loeb 2004). These authors argue that the X-ray background would be violated by a population of miniquasars if they are responsible for complete reionization. If we consider a scenario where miniquasars exist with stars, with a seed miniquasar mass fraction of 10%, we find that the X-ray background constraint at 1 keV is not violated by this miniquasar population even in the extreme case where the spectrum is normalized to the Eddington-limit. Interestingly, the level of the IRB background from the same population is consistent with current observations. Given the uncertainties in the available observations and in our analytical model, we are not yet able to exactly establish the allowed seed mass fraction.

Although current observations of the IRB are still uncertain, one can improve the limit related to the mass fraction of seed black holes further by future background measurements. In Fig. 3(c), we show the 1σ noise, or detection, level related to a planned low-resolution spectroscopic background measurement on a rocket experiment (T. Matsumoto, private communication) for IRB fluctuation studies (e.g., Magliocchetti et al. 2003; Cooray et al. 2004). The detection limit comes from the addition of 400 spectra over a 30 second integration time at an altitude above 300 km (which removes the air-glow) and after a foreground source subtraction down to 14, 15.9 and 16.3 magnitudes in I-, J- and K-bands. The background can be measured to a level of $1 \text{ nW m}^{-2} \text{ sr}^{-1}$, whereas the limiting factor in these measurements will be related to the removal of the zodiacal light (e.g., Cambrésy et al. 2001). In this case of the rocket experiment, this removal is achieved with data taken as a function of the latitude such that, when combined with multifrequency aspect, removal down to the instrumental noise level is expected. The proposed measurement would help establish the excess above Galactic stars and foreground sources better than what is currently known and, in return, limit the extent to which high- z sources, either in the form of stars and/or miniquasars, may be present.

2.4 Far-Infrared background

One may consider the possibility whether the constraint from the IRB can be relaxed if the rest UV and optical emission from miniquasars is heavily absorbed by dust. First, we note that the extinction by inter-galactic dust is unimportant at $z > 10$ even if nearly all the first stars die as pair-instability supernovae (see Yoshida et al. 2004). If the inter-stellar absorption due to dust within (proto-)galaxies that are hosting miniquasars is significant, the reradiation by thermal dust at far-IR wavelengths at $\sim 100 \mu\text{m}$ and above can still be used to put limits on their abundance. Assuming the same spectrum as shown in Fig. 2 for quasars, which allows for significant dust absorption, we predict a $850 \mu\text{m}$ background of $\sim 50 \text{ nW m}^{-2} \text{ sr}^{-1}$, for $f_{\text{BH}} = 5\%$ while the observed background is below a few $\text{nW m}^{-2} \text{ sr}^{-1}$ (Hauser

& Dwek 2001). This suggests that even for the 5% seed mass case, which may explain the missing IRB, absorption by dust cannot be as significant as for low redshift luminous quasars. Keeping the same seed mass fraction, one can refine the extent to which dust absorption is significant by studying the unresolved background at these far-IR wavelengths. While $\sim 40\%$ of the $850 \mu\text{m}$ and $350 \mu\text{m}$ backgrounds have now been resolved, the counts are such that a small extrapolation to a slightly lower flux density resolves the whole background (Borys et al. 2003). Unlike the near-IR background where surface brightness converges down to AB magnitudes of ~ 25 , as observed counts go deeper, such a convergence is not found at far-IR wavelengths. Thus, it'll be useful to return to this aspect in the future when source counts are well defined. As an early conclusion, we are forced to consider the possibility that the far-IR background can be fully explained with resolved source counts alone. This, when combined with IRB measurements, suggests that a substantial population of “dusty” miniquasars is unlikely to be present at $z > 10$.

3 SUMMARY

The cosmic infrared background (IRB) at wavelengths between $1 \mu\text{m}$ and $3 \mu\text{m}$ provides a useful probe of the global star-formation rate prior to and during the reionization. We have studied the relative contributions from first stars, supernovae and early miniquasars to the infrared background (IRB). In addition to massive stars, the IRB flux may be dominated by a population of miniquasars, especially if the first generation of stars are very massive and the end product of the stars lead to a substantial population of black holes that will effectively radiate as miniquasars by matter accretion.

We use the Press-Schechter formalism that describes dark halo formation, and combine it with a simple star-formation model to calculate the cosmic star-formation history, the supernova rate, and the blackhole formation rate at high redshift. We follow previous calculations of the source spectrum for stars, while for Population III supernovae, we use a simple description of the peak emission and its duration. We describe the flux spectrum of miniquasars using an average spectrum as observed for luminous quasars at redshifts less than 5 based on observed data and models by Sazonov et al. (2004). We fix the freedom related to the overall normalization of this spectrum by assuming that the miniquasars radiate efficiently at the maximum allowed by the Eddington-limit. Under this assumption, we find that a mass fraction of seed black holes, relative to Pop III stars, at the level of $\sim 10\%$ and below is consistent with observations. This upper limit on the seed mass fraction can naturally be extended to a higher value if miniquasars radiate below the Eddington-limit, so the limit we derive should be considered as on the lower side rather than a strict upper limit. Future spectroscopic background measurements exploiting rockets will improve the observational uncertainties and hence the constraints on the high-redshift miniquasar population.

While the integrated light from Population III supernovae to the IRB is subdominant, one can potentially consider the possibility of directly detecting individual super-

novae in high resolution deep IR imaging data. Given the star formation rate density and the expected flux, we estimate the surface density of supernovae to be order few tens per squr. degree over a year, if the star-formation rate is close to $0.5 \text{ M}_\odot \text{ yr}^{-1} \text{ Mpc}^{-3}$ at $z \sim 10$, and assuming that all stars are massive ($> 100 \text{ M}_\odot$). For the high redshift supernovae, the typical AB magnitudes are at the level of 26 in $1.5 \mu\text{m}$ (Heger et al. 2002). These are within reach of deep IR imaging with existing large telescopes and from space and, in the long term, clearly within reach of missions such as the James Webb Space Telescope (JWST), which can detect point sources down to a magnitude limit of 31 around the same wavelengths in a 10^4 sec exposure in its 16 arcmin² field of view¹.

Acknowledgments: This work is supported by the Sherman Fairchild foundation and DOE DE-FG 03-92-ER40701 (AC). NY thanks support from Japan Society of Promotion of Science Special Research Fellowship (02674). We thank an anonymous referee for a careful reading of the manuscript and for detailed comments that improved the discussion in this paper.

REFERENCES

Abel, T., Bryan, G. L., & Norman, M. L. 2002, *Science*, 295, 93
 Barkana, R. & Loeb, A. 2001, *Physics Reports*, 349, 125
 Bernstein, R. A., Freedman, W. L., Madore, B. F. 2002, *ApJ*, 571, 107
 Bond, J. R., Carr, B. J. & Hogan, C. J. 1986, *ApJ*, 280, 825
 Borys, C., Chapman, S., Halpern, M. & Douglas, S. 2003, *MNRAS*, 344, 385
 Bromm, V., Kudritzki, R. P. & Loeb, A. 2001, *ApJ*, 552, 464
 Bromm, V., Coppi, P. S., & Larson, R. B., 2002, *ApJ*, 564, 23
 Cambrésy, L., Reach, W. T., Beichman, C. A., & Jarrett, T. H. 2001, *ApJ*, 555, 563
 Carr, B. J., Bond, J. R., & Arnett, W. D. 1984, *ApJ*, 277, 445
 Cen, R., 2003, *ApJ*, 591, 12
 Chen, X., Cooray, A., Yoshida, N., & Sugiyama, N. 2003, *MNRAS*, 346, L31
 Cooray, A., Bock, J. J., Keating, B., Lange, A. & Matsumoto, T. 2004, *ApJ*, 606, 611
 Dijkstra, M., Haiman, Z. & Loeb, A. 2004, *ApJ* submitted (astro-ph/0403078).
 Fukugita, M. & Kawasaki, M. 2003, *MNRAS*, 343, L25
 Hauser, M. & Dwek, E. 2001, *ARAA*, 39, 249
 Haiman, Z., & Loeb, A. 1998, *ApJ*, 503, 505
 Heger, A., & Woosley, S. E. 2002, *ApJ*, 567, 532
 Heger, A., Woosley, S. E., Baraffe, I. & Abel, T. 2002, in: Gilfanov, M. et al. eds. "Lighthouses of the Universe: The Most Luminous Celestial Objects and their use for Cosmology", Springer-Verlag, Berlin [preprint astro-ph/0112059]
 Hernquist, L. & Springel, V. 2003, *MNRAS*, 341, 1253
 Kashlinsky, A. et al. 2004, *ApJ* in press (astro-ph/0401401)
 Kogut, A. et al. 2003, *ApJS*, 148, 161
 Loeb, A. & Rybicki, G. B. 1999, *ApJ*, 524, 527
 Machacek, M. E., Bryan, G., & Abel, T. 2003, *MNRAS*,
 Madau, P., Rees, M. J., Volonteri, M., Haardt, F., & Oh, S.-P. 2004, *ApJ*, 604, 484
 Magliocchetti, M., Salvaterra, R., & Ferrara, A. 2003, *MNRAS*, 342, L25
 Pozzetti, L. & Madau, P. 2000, in *The Extragalactic Infrared Background and its Cosmological Implications*, eds. M. Hartwig & M. G. Hauser (ASP: San Francisco).
 Press, W. H., & Schechter, P. 1974, *ApJ*, 187, 425 [PS]
 Ricotti, M., & Ostriker, J. P. 2003, *MNRAS* in press (astro-ph/0311003).
 Salvaterra, R. & Ferrara, A. 2003, *MNRAS*, 339, 973
 Santos, M. R., Bromm, V., & Kamionkowski, M. 2002, *MNRAS*, 336, 1082
 Sazonov, S. Yu., Ostriker, J. P., & Sunyaev, R. A. 2004, *MNRAS*, 347, 144
 Schaefer, D. 2002, *A&A*, 382, 28
 Schaefer, D. 2003, *A&A*, 397, 527
 Sokasian, A., Yoshida, N., Abel, T., Hernquist, L., & Springel, V. 2004, *MNRAS*, 350, 47
 Steidel, C. C., Hunt, M. P., Shapley, A. E., Adelberger, K. L., Pettini, M., Dickinson, M. & Giavalisco, M. 2002, *ApJ*, 576, 653
 Sunyaev R. A., Zel'dovich Ya. B., 1980, *ARAA*, 18, 537
 Tegmark, M., Silk, J. R., Rees, M. J., Blanchard, A., Abel, T., Palla, F. 1997, *ApJ*, 474, 1
 Tegmark, M., Strauss, M. A., Blanton, M. R., Abazajian, K., Dodelson, S., Sandvik, H., Wang, X., et al. 2004, astro-ph/0310723
 Totani, T., Yoshii, Y., Iwamuro, F., Maihara, T. & Motohara, K. 2001, *ApJ*, 550, L137
 Venkatesan, A., Tumlinson, J. & Shull, M. J. 2003, *ApJ*, 584, 621
 Wyithe, S. & Loeb, A. 2003, *ApJ*, 588, L69
 Wright, E. L. & Johnson, B. D. 2001, preprint astro-ph/0107205
 Yoshida, N., Abel, T., Hernquist, L. & Sugiyama, N. 2003, *ApJ*, 592, 495
 Yoshida, N., Bromm, V. & Hernquist, L. 2004, *ApJ*, 605, 579

¹ <http://www.ngst.nasa.gov> for sensitivities and other details